Journal of Semiconductors
JOS iopscience.iop.org/jos
www.jos.ac.cn

Recent progress on elemental tellurium and its devices

Jiachi Liao, Zhengxun Lai, You Meng, and Johnny C. Ho

Citation: J C Liao, Z X Lai, Y Meng, and J C. Ho, Recent progress on elemental tellurium and its devices[J]. *J. Semicond.*, 2025, 46(1), 011605.

View online: https://doi.org/10.1088/1674-4926/24090020

REVIEWS

Journal of Semiconductors, 2025, 46, 011605
DOI: 10.1088/1674-4926/24090020
CSTR: 32376.14.1674-4926.24090020

Recent progress on elemental tellurium and its devices

Jiachi Liao[1], Zhengxun Lai[2], You Meng[1, 2, †], and Johnny C. Ho[1, 3, 4, †]

[1]Department of Materials Science and Engineering, City University of Hong Kong, Kowloon, Hong Kong 999077, China

[2]Changsha Semiconductor Technology and Application Innovation Research Institute, College of Semiconductors (College of Integrated Circuits), Hunan University, Changsha 410082, China

[3]Institute for Materials Chemistry and Engineering, Kyushu University, Fukuoka 8168580, Japan

[4]State Key Laboratory of Terahertz and Millimeter Waves, City University of Hong Kong, Kowloon, Hong Kong 999077, China

Abstract: The rapid advancement of information technology has heightened interest in complementary devices and circuits. Conventional p-type semiconductors often lack sufficient electrical performance, thus prompting the search for new materials with high hole mobility and long-term stability. Elemental tellurium (Te), featuring a one-dimensional chiral atomic structure, has emerged as a promising candidate due to its narrow bandgap, high hole mobility, and versatility in industrial applications, particularly in electronics and renewable energy. This review highlights recent progress in Te nanostructures and related devices, focusing on synthesis methods, including vapor deposition and hydrothermal synthesis, which produce Te nanowires, nanorods, and other nanostructures. Critical applications in photodetectors, gas sensors, and energy harvesting devices are discussed, with a special emphasis on their role within the internet of things (IoT) framework, a rapidly growing field that is reshaping our technological landscape. The prospects and potential applications of Te-based technologies are also highlighted.

Key words: elemental tellurium; photodetector; field-effect transistor; gas sensor; energy harvesting device

Citation: J C Liao, Z X Lai, Y Meng, and J C. Ho, Recent progress on elemental tellurium and its devices[J]. *J. Semicond.*, 2025, 46(1), 011605. https://doi.org/10.1088/1674-4926/24090020

1. Introduction

Conventional inorganic p-type semiconductors suffer from low carrier mobility and localized valence band maximum, limiting their electrical performance. While significant research has been directed towards n-type semiconductor materials, new p-type materials have not garnered equivalent attention. Nonetheless, some new p-type materials, such as elemental tellurium (Te), exhibit higher hole mobility with excellent environmental stability. Since its discovery in 1782, Te has continually attracted scientific interest, with its physicochemical properties being extensively studied throughout the 19th century[1]. In recent decades, Te found applications in optoelectronic devices, including photoconductors and infrared detectors. In 2001 and 2007, researchers further explored the diverse properties of Te alloys and their use in gas sensors, enhancing the popularity of Te. The continuous exploration of its thermoelectric and ferroelectric properties inspires further research and development in this field[2–5].

The investigations of Te have been re-visited in recent years, establishing it as a critical semiconductor material for next-generation devices and circuits. This is attributed to the unique properties of Te, such as its photoelectric[6, 7], thermoelectric[8], and piezoelectric characteristics[9]. Unlike some nanostructures that require complex preparation processes and strict stoichiometric ratios, elemental Te stands out due to its superior physical performance. However, devices based on elemental Te still face challenges related to stability and durability, necessitating further research to ensure high mobility and air stability.

This paper reviews recent breakthroughs related to elemental Te, focusing on synthesizing nanostructures with various morphologies, the mechanisms underlying different devices' physical responses, and recent research applications. First, we reviewed elemental Te's crystal structure and intrinsic nature, emphasizing preparation methods for various orientations and shapes. After that, we discuss the prospects and challenges of recent applications, including photothermoelectric detectors (PTEs), field-effect transistors (FETs), and gas sensors. It is worth to note that several comprehensive review papers about Te-based electronics and optoelectronics have been reported before[10, 11].

2. Structure and properties of elemental Te

The crystal structure of a material determines its chemical and physical properties. Elemental Te exhibits remarkable properties, including photoelectric, thermoelectric, and photothermoelectric characteristics, attributable to its unique atomic arrangement and strong spiral structure. In this section, we will delve into Te's distinctive chain-like crystal structure and its associated properties. We will also highlight studies on the physical properties of Te, particularly in computational molecular dynamics and density-functional theory (DFT). This comprehensive examination aims to understand the better intrinsic qualities that make elemental Te a promising material for various advanced applications.

2.1. Crystal structure

The elemental Te crystal structure consists of helical

Correspondence to: Y Meng, youmeng2@cityu.edu.hk; J C. Ho, johnnyho@cityu.edu.hk

Received 10 SEPTEMBER 2024; Revised 8 OCTOBER 2024.

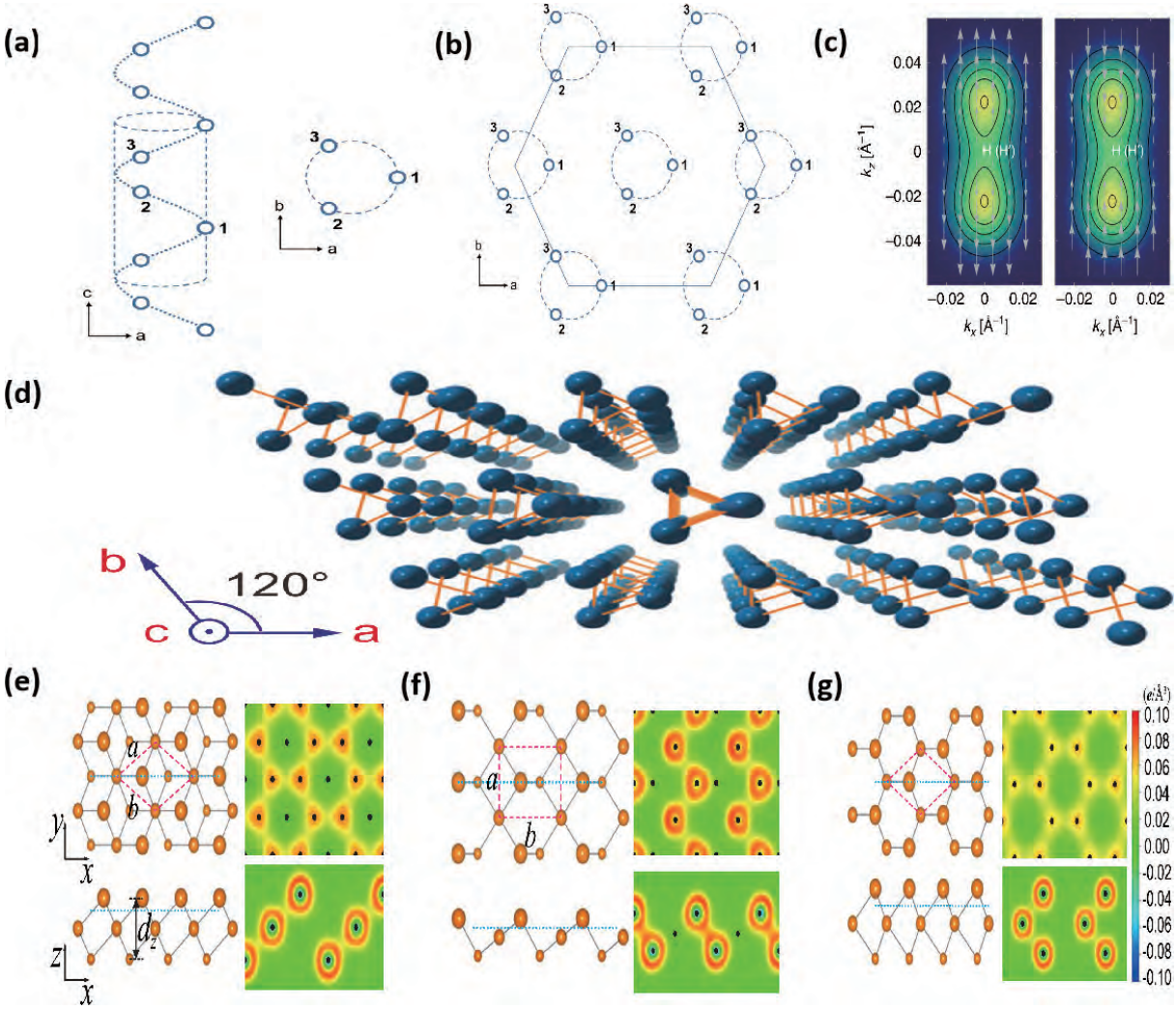

Fig. 1. (Color online) The atomic and electronic structure of elemental Te. (a) The schematic picture of the Te structure consists of helical Te chains arranged in hexagonal arrays along the *c* direction. (b) Te atoms bound together by faint van der Waals force. Adapted with permission from Ref. [16]. Copyright 2023, Nature Publishing Group. (c) For the enantiomeric structures, the helical chains are arranged in different ways related to other properties. Adapted with permission from Ref. [12]. Copyright 2017, Nature Publishing Group. (d) The three-dimensional image of the spiral structure of elemental Te. Adapted with permission from Ref. [13]. Copyright 2024, Nature Publishing Group. (e)–(g) The atomic and electronic structures of *α*-, *β*-, and *γ*-phases of elemental Te. Adapted with permission from Ref. [14]. Copyright 2017, American Physical Society.

chains of bonded atoms arranged in a hexagonal array, as shown in Fig. 1(a). Crystal Te belongs to the hexagonal crystal system and has high symmetry. In Fig. 1(b), Te atoms are combined through van der Waals forces to shape a hexagonal structure. In addition, its symmetry leads to the existence of enantiomeric forms containing opposite chiral helices, the right-handed helix belonging to the space group $P3_121$ and $P3_221$ with opposite rotational properties[12], as shown in Fig. 1(c). The three-dimensional structure of Te helical chains has been displayed in Fig. 1(d)[13]. Recently, Zhu *et al.*[14] derived that Te has three phases of two-dimensional elemental Te (*α*-Te and *γ*-Te) and tetragonal (*β*-Te) structures, which are presented in Figs. 1(e)–1(g). Both *α*- and *γ*-Te phases indicate threefold and sixfold coordination structures, respectively, while the *β*-Te phase demonstrates a hybridization of threefold and fourfold. Among these different phases, *α*-Te and *β*-Te exhibit room-temperature stability because of their higher cohesive energy (2.62 eV per atom for *α*-Te and 2.56 eV per atom for *β*-Te), while *γ*-Te, with a lower cohesive energy of 2.46 eV per atom, so is unstable above 200 K. Nowadays, Yan *et al.*[15] reported two other ultra-stable novel allotropes of Te few-layers in calculations, namely metallic *ε*- and *ζ*-phase Te few layers. The unique trilayer arrangement of Te leads to various intriguing properties of Te atoms in different layers. Te atoms in the central layer, with a higher coordination number, exhibit metallic characteristics, while the Te atoms in outer layers, with a lower coordination number, behave more like a semiconductor. The diversity of these structures leads to the versatility of elemental Te, which holds promise for device utilization.

The crystal structure also makes elemental Te comprising van der Waals-bonded one-dimensional helix Te chains[16]. It will influence the properties like light absorption and thermal conductivity. Te exhibits excellent electronic and optical properties along the plane direction, while it performs poorly perpendicular to the plane direction. Moreover, because elemental Te as a p-type semiconductor has a chiral structure, anisotropic features in terms of mechanical, thermoelectrical, and optical properties would be involved, which will be discussed in detail later.

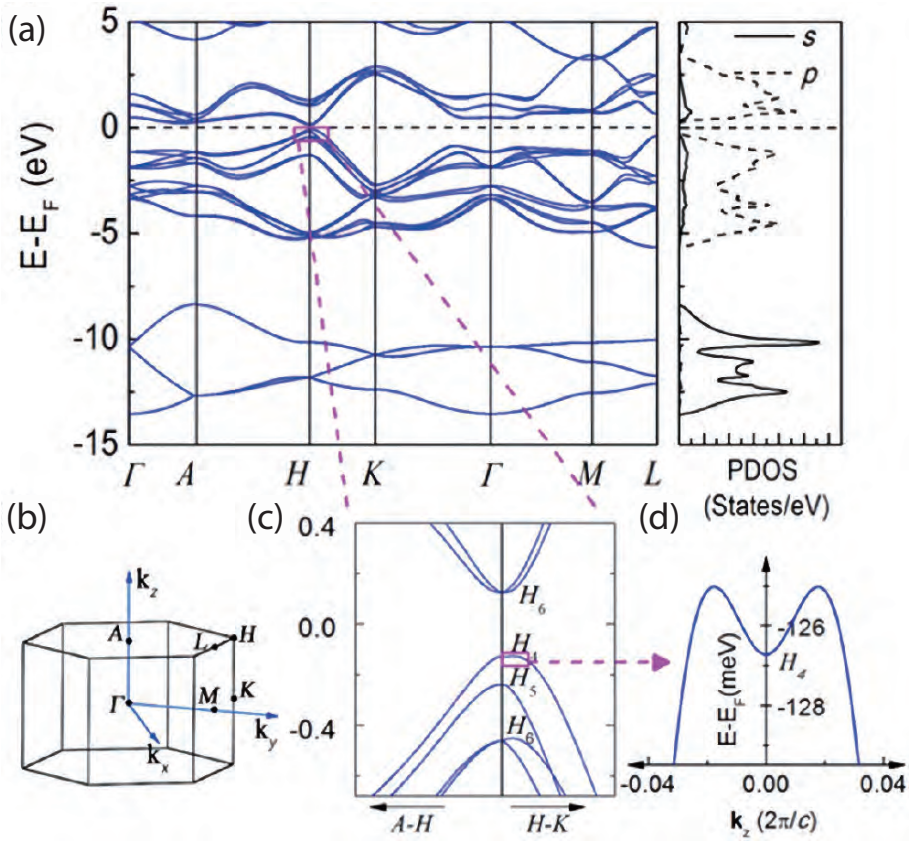

Fig. 2. (Color online) The electrical and optical properties of elemental Te. (a) Band structures of Te based on the spin–orbit (SOC) coupling and the corresponding partial density of states. (b) First Brillouin zone (BZ) of elemental Te. (c) Amplify the band characteristics near the edge of the direct band at the H point. (d) Magnify the image of the area near the VBM. Adapted the permission from Ref. [19]. Copyright 2021, Nature Publishing Group.

2.2. Electrical properties

The energy band structure of element Te has a direct bandgap between the valence and conduction bands, which determines its electrical properties[17]. Nowadays, electrical properties and energy structures have been simulated using different methods like MD simulation and DFT calculation[18]. Zhu *et al.*[14] reported a single-layer 2D Te with a direct bandgap of 1.04 eV obtained using the first principle calculation. In addition, to explore the effect on elemental Te bandgap under different strain conditions and confirm that the bandgap can be adjusted with the external strain. They discovered that when the tensile strain was uploaded on the *c*-axis of the Te helical chains up to 6%, the minimum point of the conduction band (CB) gradually decreased roughly from 0.7–0.5 eV towards the Fermi energy level. On the contrary, the maximum point of the valence band (VB) remains almost unchanged at −0.25 eV approximately. As a result, the bandgap decreases to 0.86 eV at 6% of the tensile strain condition. However, when the content of the strain is at 10%, the VBM undergoes an imbalance, demonstrating that the device is already experiencing performance damage.

Due to the helical crystal structure, elemental Te gives rise to isotropic band dispersion around the Fermi energy levels. Recently, Qiu *et al.*[19] also calculated the energy band structure and the coupling of the spin–orbit (SOC) Te, as demonstrated in Fig. 2(a). In addition, it can be clearly viewed that the Dirac cone dispersion occurs at P1 in the Brillouin zone (BZ). This helical structure makes the material strictly anisotropic in the crystal orientation. According to the band structure and spin–orbit coupling of 2D Te, it can be seen from Fig. 2(c) that elemental Te can be proved as a direct bandgap material with a bandgap energy of about 0.32 eV. Qiao *et al.*[17] also calculated the band structure of few layers Te and performed ab initio simulations based on DFT calculations. They found that as the number of Te layers increased, the bandgap decreased from 1.17 eV for 2-layer Te to 0.66 eV for 6-layer Te. Although the bandgap exhibits variations in different works, it reveals a consistent common trend: the bandgap decreases with increasing Te layers.

2.3. Optical properties

Through external light excitation, the electrons in the VB can cross the forbidden band to reach the CB, becoming free electrons capable of transport. According to those above, elemental Te has a direct bandgap and a width of about 0.32 eV. This allows the Te device to be adjusted to absorb light at different wavelengths (broad spectral response) and other advantages compared with the traditional indirect semiconductors[20]. This determines its photoelectric conversion efficiency, by which the photodetection performance is thus determined. Due to its narrow bandgap, Te-based optoelectronics has broad spectral absorption and can absorb a broad spectrum from ultraviolet to infrared light. The optical properties of Te materials have led to an enormous scope of applications in photoelectric devices, optical components, photovoltaic conversion, and other fields.

2.4. Thermoelectric properties

As internal combustion engines continue to be inno-

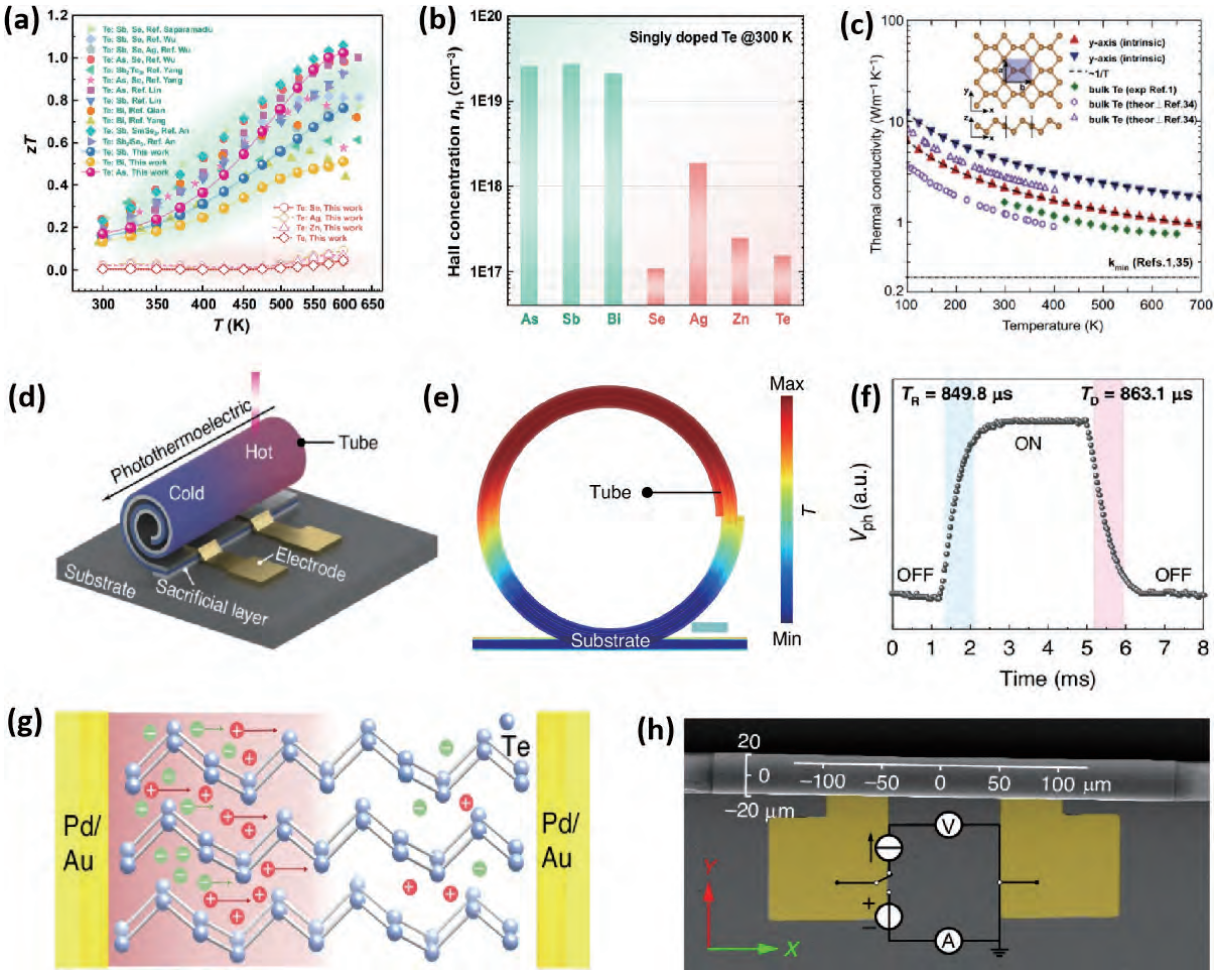

Fig. 3. (Color online) The thermoelectric properties of elemental Te and Te-based devices. (a), (b) The thermoelectric performance and Hall concentration based on different doped Te devices. Adapted with permission from Ref. [27]. Copyright 2024, Nature Publishing Group. (c) Temperature dependence of Te lattice thermal conductivity. Adapted with permission from Ref. [25]. Copyright 2018, Royal Society of Chemistry. (d)–(h) The performance and schematic images of a self-rolled tubular Te device. Adapted with permission of Ref. [29]. Copyright 2024, Nature Publishing Group.

vated and retrofitted, factories are putting more effort into the efficiency of waste heat utilization, so it is essential to manufacture devices with thermoelectric capability. Thermoelectric technology improves the utilization of waste heat from factories and other places and converts it into current and vice versa. Elemental Te, graphene[21], germanium[22–24], and other materials have attracted much attention in thermoelectric applications.

The thermoelectric properties of a material are judged by the following formula, $ZT = S^2\sigma T/(K_E + K_L)$, where S, σ, K_E, K_L, and T represent the seebeck coefficient, electrical conductivity, electronic thermal conductivity, lattice thermal conductivity, and temperature, respectively. Since the electrical properties, including S, σ, and K_E are intimately coupled with each other, a straightforward refinement of one of these parameters usually results in compensation for the other, leading to difficulties in enhancing the thermoelectric properties of the device this year.

In 2018, Gao *et al.*[25] theoretically obtained the thermal and thermoelectric properties of elemental Te nanosheets through first principle calculations. According to the calculations, two-dimensional Te has an extremely low lattice thermal conductivity at room temperature, representing 2.16 W·m^{-1}·K^{-1}, much lower than its body thermal conductivity. Fig. 3(c) displays the relationship of K_L with the temperature. In addition, Lin *et al.* proposed that the thermoelectric properties of the element Te can be improved by inducing doping and precipitation with Sb[26]. The substitution of Sb in Te within 0.5% is sufficient to increase the hole concentration and optimize the thermoelectric power factor, achieving effective phonon scattering and reducing lattice thermal conductivity by about 25%. This study further confirms that Te is a promising elemental thermoelectric material with a temperature range of 300 to 650 K. As shown in Figs. 3(a) and 3(b), doped Te and related telluride perform well in improving the thermoelectric properties of elemental Te, being promising in the field of thermoelectric technology[27]. The effective phonon scattering and reduction in lattice thermal conductivity are practical implications of this research, providing reassurance about the potential applications of elemental Te in the field of thermoelectric technology.

2.5. Photothermoelctric properties

Recently, the photothermoelectric (PTE) effect has gained significant attention for use in broad-spectrum detectors. Specifically, when Te devices are irradiated by near-infrared or visible light, a temperature gradient is generated across the device. The energy of the photon is sufficient to cross the

Table 1. The material property and environmental stability of different material devices.

Materials	Mobility ($cm^2/(V·s)$)	Stability
Te[2] (Direct bandgap, 0.35–1.265 eV)	~10^3	2 months
MoS_2[37, 38] (Indirect bandgap, 0.75–1.89 eV)	480	3 months
Black phosphorus[39] (Direct bandgap, 0.3–1.5 eV)	~10^3	50 hours
WS_2[40, 41] (Indirect bandgap, 0.75–1.91 eV)	970	2 weeks
Bi_2Se_3[31] (Direct bandgap, 0.2–0.3 eV)	1000–4000	6 months
WSe_2[42, 43] (Indirect bandgap, 0.90–1.54 eV)	~500	1 month
$MoSe_2$[44, 45] (Indirect bandgap, 0.80–1.58 eV)	~50	21 days

narrow bandgap of the Te device and is thus absorbed, leading to a localized temperature rise. The temperature difference can result in electrons and holes migrating in response to temperature gradients, creating an electric field that is subsequently converted into the output signal. A notable example of such an application is the development of a self-power, wideband PTE detector using an elemental Te channel[28]. This device surpasses the limitations imposed by the energy bandgap, enabling operation at wavelengths up to approximately 10.6 μm. Remarkably, it exhibits a short response time of 8.3 ms and a recovery time of 8.8 ms, along with high detectivity at room temperature[29]. Developing such high-performance PTE-based detectors underscores the potential of elemental Te in advanced broad-spectrum optoelectronic applications.

Furthermore, to overcome the limitations of polarization sensitivity caused by insufficient photon-to-electron conversion, Dai *et al.* experimentally developed a miniaturized detector using one-dimensional Te nanoribbons[30]. This design can be adjusted to significantly enhance the PTE response to polarization-sensitive absorption, leveraging a plasmonic absorber. This device offers a prospective alternative for miniaturized room-temperature infrared photodetectors with considerable polarization sensitivity[30]. Comparing the performance with the PTE detector based on Bi_2Se_3[31], the elemental Te device performs better, with faster response time, higher response photovoltage, and stable operation. For example, Huang *et al.*[29] reported a three-dimensional PTE detector based on a self-rolled tubular Te (TTD), as shown in Fig. 3(d). The unique device structure makes it more promising for a PTE detector, as shown in Fig. 3(e), by which the TTD better localizes the thermal energy. As a result, the temperature difference between the two ends of the device will be further increased, realizing the power transfer from the hot side to the cold side. The localization of light energy in the elemental Te layer with an elevated refractive index is observed despite an air gap between neighboring spins. In Fig. 3(f), the fast photoresponse of the TTD is demonstrated, having a rise time of 849.8 μs and a decay time of 863.1 μs.

2.6. Stability

For many traditional p-type materials and some two-dimensional (2D) materials, such as perovskites, black phosphorus, and transition metal dichalcogenides (TMDCs)[32–35], stability has been a significant obstacle to practical production. In contrast, Te-based devices exhibit excellent environmental stability, primarily due to energy barriers in the oxidation pathway, which prevent moisture and oxygen in the air from disrupting the devices' integrity. Additionally, Te nanostructures grown on flexible substrates also demonstrate bending stability[16].

However, the thermal instability of Te-based devices has not been thoroughly investigated, which poses a significant drawback for their practical applications. To address this issue, Zhao *et al.*[36] examined the effect of annealing temperature on Te thin-film transistors and identified two failure mechanisms: the sublimation of Te channels and the degradation of contacts. To mitigate these issues, they developed a method to contact the Te device with graphene and encapsulate it with SiO_x. This approach ensures that the Te channel and contacts remain intact and stable at high temperatures.

According to Table 1, elemental Te is competitive in both hole mobility and environmental stability. Additionally, Meng *et al.*[16] have also demonstrated the bending stability and long-term performance stability of Te-based devices. The device maintains a good photoresponse even after over 5000 bending cycles, with the photocurrent remaining consistent with the initial measurements. These results highlight the operation and environmental stability of elemental Te. The test performance and stability indicate that elemental Te nanostructures hold significant potential for applications in electronic and optoelectronic utilization.

3. Synthesis of Te nanostructures

Unlike other emerging semiconductor materials, elemental Te is less expensive to prepare because pre-mixing and pre-processing are not required for crystalline Te materials. Furthermore, the single-element Te eliminates the need to control the dosage of each chemical component and the stoichiometric ratio. In this section, we will focus on introducing the synthesis of typical nanostructures using major methods such as physical vapor deposition (PVD), chemical vapor deposition (CVD), hydrothermal synthesis, and so on.

3.1. Physical/chemical vapor deposition of Te nanostructures

To produce ultrathin Te nanoflakes, the PVD synthesis method typically requires a vacuum environment and high-purity sources. A recent study conducted by Apte *et al.*[46] utilized this method to investigate the synthesis of ultrathin Te nanoflakes with a thickness of less than 7 nm and a size of 50 μm, as shown in Fig. 4(a). Under a growth temperature of 650 °C and Ar carrier gas, the synthesized Te nanoflakes have a thickness down to 0.85 nm, corresponding to three atomic layers (Fig. 4(b)). PVD can also be used for the growth of one-dimensional Te nanostructures in which Te microrods were deposited at temperatures roughly 400 °C under 1 atm pressure. In comparison, nanotubes were deposited at lower temperatures, less than 200 °C[47]. The growth of elemental Te nanostructures is observed to follow the nucleation of spheri-

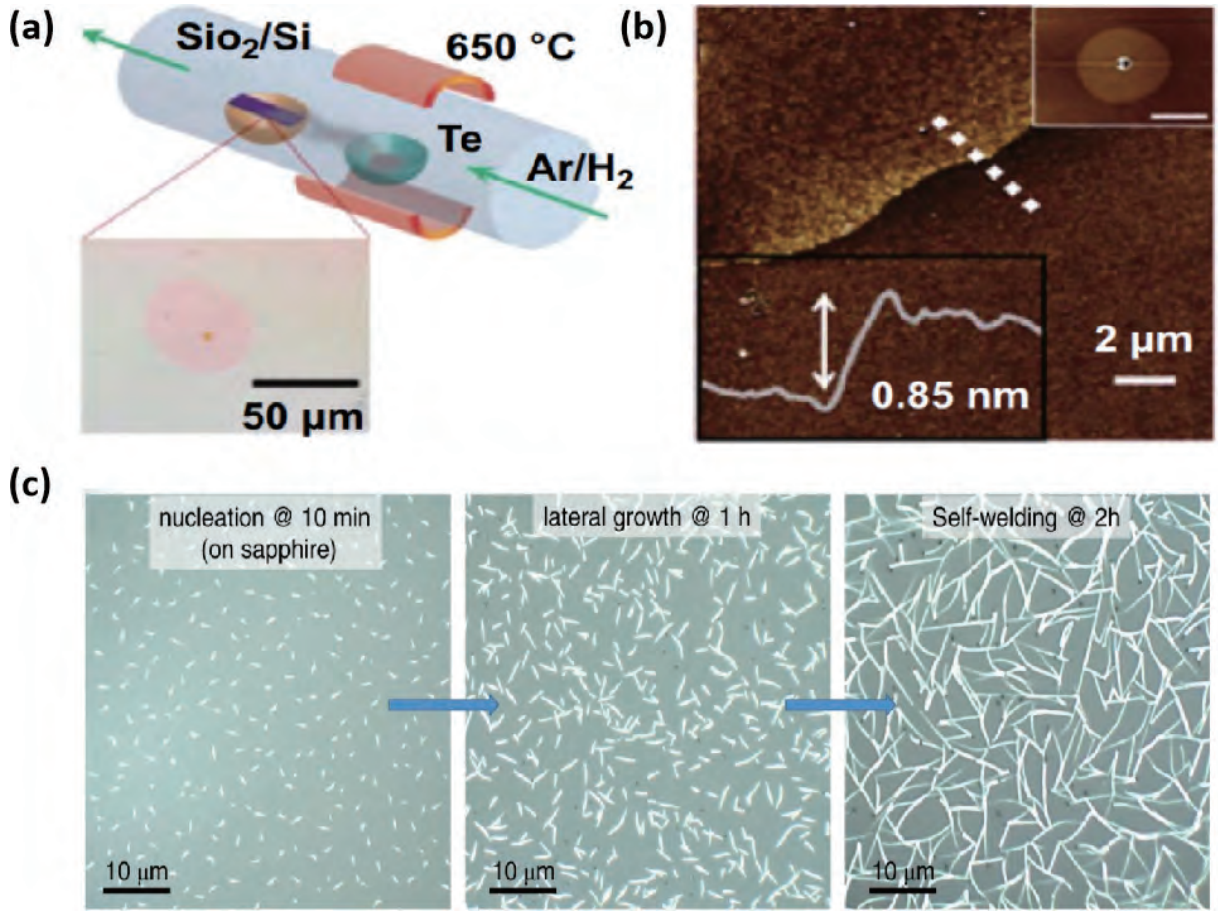

Fig. 4. (Color online) PVD and CVD process of Te nanostructures. (a) Schematic illustration of the CVD synthesis process of Te nanostructure. (b) The AFM image of elemental Te nanoflake. Adapted with permission from Ref. [46]. Copyright 2019, IOP Publishing. (c) The morphological changes of Te nanomesh with different growth times. Adapted with permission from Ref. [16]. Copyright 2023, Nature Publishing Group.

cal particles, followed by the growth of one-dimensional structures. The nanostructures may have different growth morphologies and orientations due to various growth temperatures, carrier gas flow, and growth duration.

CVD is another commonly used method for synthesizing nanostructures. It involves depositing nanomaterials onto a solid surface through a gas phase reaction. Unlike PVD, CVD typically relies on chemical reactions among carrier gas, source, and catalyst. In the case of Te nanowire synthesis, the Te source can be carried by a carrier gas and then passed to a specific catalyst at certain growth temperatures, forming nanostructures on a solid surface. Te nanostructures with different morphologies and orientations were successfully prepared by modulating the experimental parameters such as temperature, pressure, and precursor concentration. Recently, Meng *et al.*[16] used the CVD process to synthesize Te nanomesh at 100 °C, where atmospheric pressure is used for the growth of Te nanomesh in this work, as shown in Fig. 4(c). With prolonged growth duration, the Te nanomesh structure gradually forms through a self-welding process, exhibiting excellent connectivity. The resulting samples were then subjected to morphological, structural, and compositional analysis to examine the impact of various conditions on the formation of Te nanostructures. In addition, Xu *et al.*[48] identified that hydrogen plays an essential role in the growth of Te nanoribbons during CVD preparation. In their experiments, they introduced hydrogen during the growth of Te nanoribbons and found that hydrogen effectively reduced the formation of defects and impurities in Te nanoribbons. These improvements led to a substantial increase in the hole mobility of the Te nanoribbons through detailed transport measurements and field-effect transistor experiments. CVD offers high purity, controllability, and suitability for large-area growth. However, preparing elemental Te nanostructures using CVD comes with a high instrumentation cost and is highly sensitive to the substrate conditions.

3.2. Van der Waals epitaxy

Van der Waals epitaxy (vdWE) growth has gained significant attention due to its wide range of applications in synthesizing various vdW layered materials. vdWE synthesis can overcome large lattice mismatches and facilitate the movement of adsorbed atoms of vdW materials along the substrate surface. Furthermore, the vdWE method allows the upper layer to relax perfectly, disregarding any heterogeneous interfacial strain. Recently, vdWE growth has been used to synthesize 2D Te on mica substrates by Wang *et al.*[49], the resulting 2D Te nanoflakes grown on mica substrates have large lateral dimensions and hexagonal crystallinity, supported by the TEM study. In addition, 2D Te nanoflakes with single and few-layer thicknesses were successfully synthesized on graphene substrates. The Te nanostructures obtained by molecular beam epitaxy were shown using material structure characterization to have their helical chains in parallel with the graphene substrate. Compared to the $CsPbBr_3$ perovskite nanowires synthesized through vdWE growth by Li *et al.*[50],

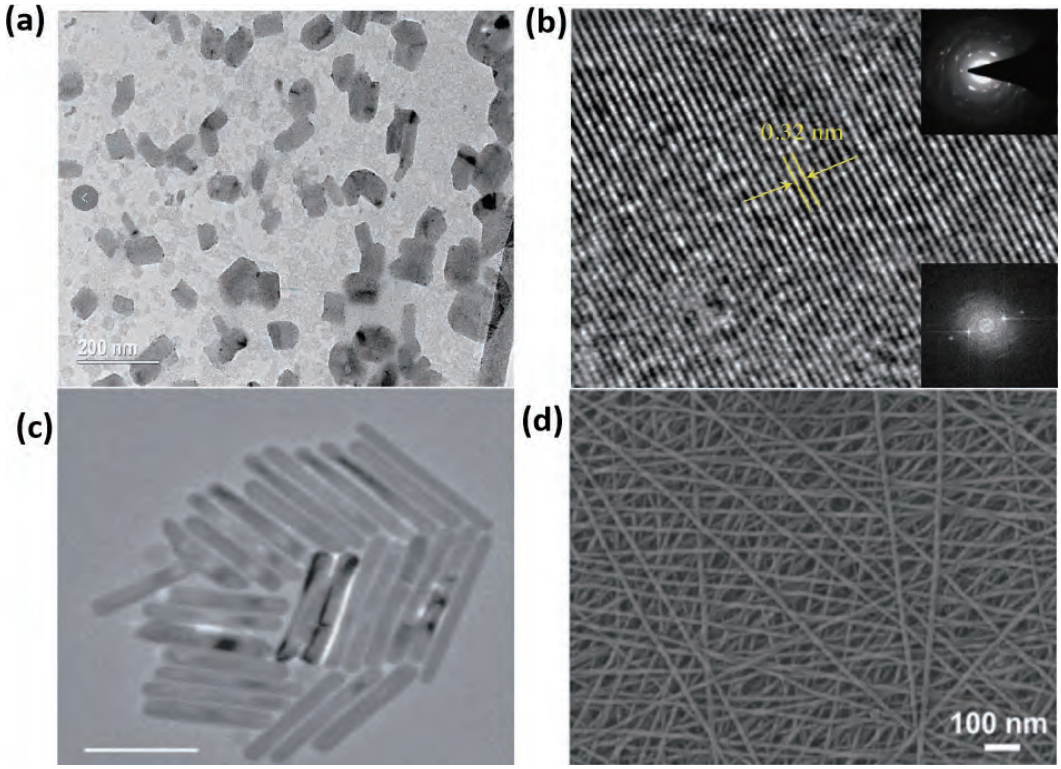

Fig. 5. (Color online) The morphology of different elemental Te nanostructures. (a), (b) The TEM images of 2D Te nanoflakes. Adapted with permission of Ref. [52]. Copyright 2018, WILEY-VCH. (c) The TEM image of Te nanorods. The scale bar is 100 nm. Adapted with permission of Ref. [53]. Copyright 2014, Nature Publishing Group. (d) The SEM image of Te nanonet. Adapted permission with of Ref. [54]. Copyright 2021, Nature Publishing Group.

the preparation of 2D Te nanoflakes does not require consideration of the elemental distribution during the preparation process. This highlights the advantage of the simplicity in preparing Te nanostructures. The method is also applied for the growth of tellurides, such as the preparation of ultrathin (~ 4.8 nm) single-crystalline CdTe nanosheets using the vdWE growth technique proposed by Cheng *et al*.[51]. Recently, Xie *et al*.[52] obtained high-quality 2D Te nanostructures by a liquid-phase exfoliation method, by which the TEM images in Figs. 5(a) and 5(b) show the interplanar spacing of crystalline Te nanoflake. Also, Ben-Moshe *et al*.[53] used TEM study to observe different morphologies of Te nanorods grown by controllable reduction of Te cations, as shown in Fig. 5(c).

3.3. Hydrothermal synthesis

Hydrothermal synthesis is a widely used method for preparing nanomaterials through chemical reactions in an aqueous solution at high temperature and pressure inside an autoclave. Back in 2002, Mo *et al*.[55] successfully synthesized thin single-crystal Te nanoribbon nanotubes by a controlled hydrothermal synthesis method, and achieved precise control of the morphology and size of the Te nanostructures by adjusting the reaction conditions and adding surfactants during the preparation process. Detailed material characterization and structural analysis determined the crystal structures and growth mechanisms of the synthesized nanoribbons and nanotubes. This study provides a new approach and understanding of the precise synthesis of Te nanostructures and lays the foundation for their application in nanoelectronics and optoelectronics. The hydrothermal method has a well-established processing pathway for preparing Te nanowires. For example, hydrothermal synthesis can be used to obtain single-crystal Te nanowires with an average diameter of 70 nm and Te/C nanocables with a diameter ranging from 50–100 nm. This is achieved by reducing Na_2TeO_3 with glucose in the presence of cetyltrimethylammonium bromide (CTAB) under hydrothermal conditions at temperatures of 130–170 °C. In the hydrothermal process, temperature was found to play an essential role in determining the resulting Te nanowires and Te/C nanocables. The hydrothermal method offers a low-cost, low-energy, and relatively simple process for producing pure Te nanowires in large quantities. Recently, Naqi *et al*.[54] used a hydrothermal method to prepare elemental Te nanonet at a relatively low temperature using polyvinylpyrrolidone (PVP) as a capping agent. At the same time, the corresponding SEM image can be found in Fig 5(d). However, high temperatures, high pressures, and extended growth duration are usually needed in a hydrothermal synthesis, which affects productivity and increases energy consumption.

3.4. Thermal evaporation of Te-based films

Thermal evaporation is a widely adopted technique for optoelectronic devices, solar cells, thin-film transistors, and other fields. This method involves heating the source material in a high vacuum until it reaches its vaporization temperature. The evaporated source then diffuses and settles on the substrate surface within the vacuum chamber, forming a thin film. In the initial stage, Te thin films were deposited on glass and alumina substrates for NO_2 gas sensor applications. The surface morphology and structure of these deposited Te films were examined using techniques such as scanning electron microscopy (SEM), X-ray diffraction (XRD), and raman spectroscopy. The morphology of the films varied from amor-

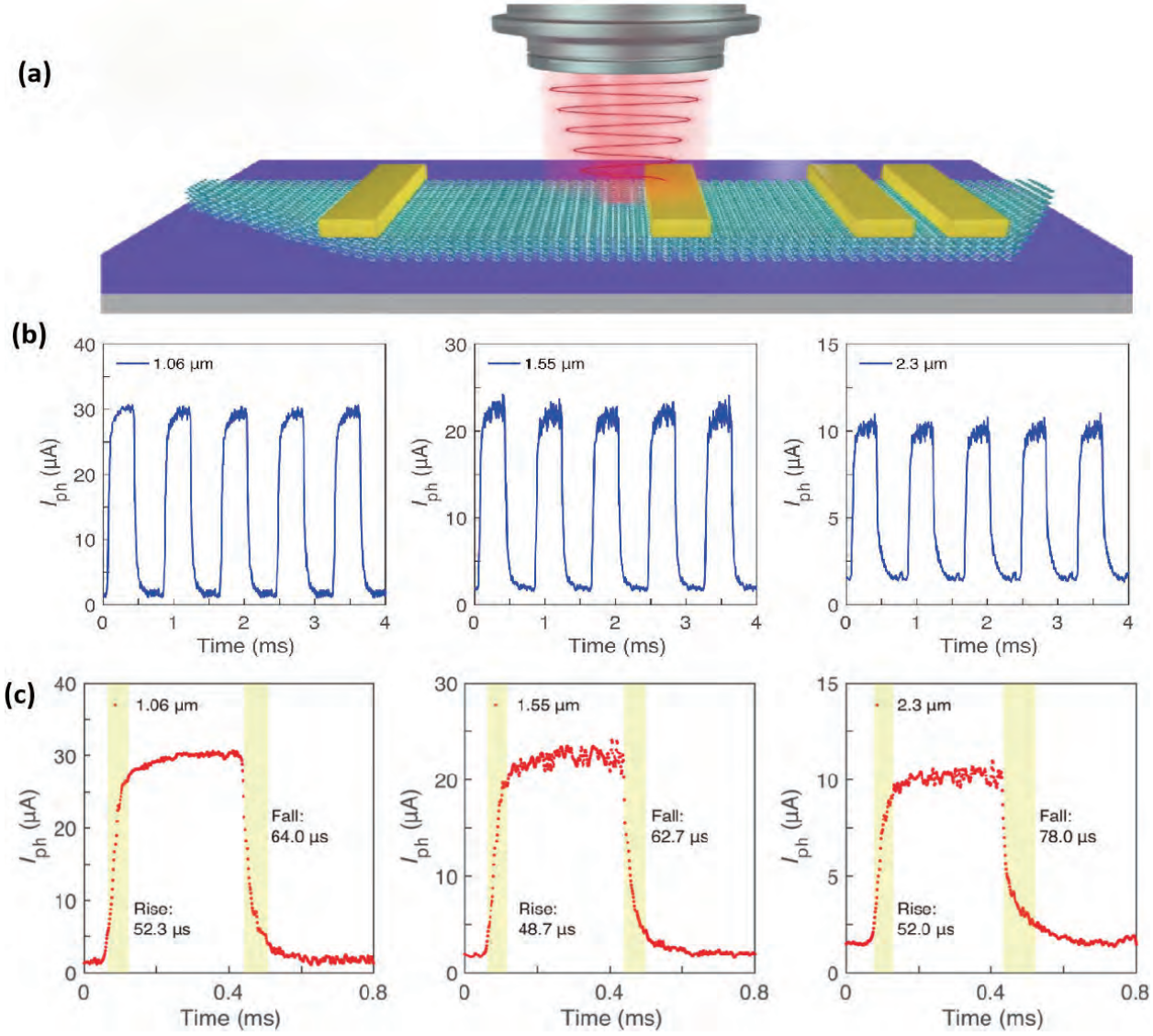

Fig. 6. (Color online) The photodetector based on elemental Te. (a) The schematic picture of the photodetecting device. (b), (c) The photocurrent response, including rise and fall time, based on quasi-2D Te under different light wavelengths. Adapted permission with Ref. [73]. Copyright 2020, Nature Publishing Group.

phous to polycrystalline as the film thickness increased from 100 to 300 nm[56].

The deposition temperature and subsequent annealing steps significantly influence the thermal expansion process of Te thin films. Controlling these parameters is crucial to achieving a desirable morphology and orientation of the elemental Te thin film. For instance, Okuyama *et al*.[57] studied the effect of substrate temperature on the crystallinity and electronic properties of thermal evaporated Te thin films on glass substrates. Their findings revealed that the grain size of the films increases with higher substrate temperatures. Conversely, when the substrate temperature is below 188 K, the grain size decreases. This suggests that Te thin films synthesized at temperatures below 323 K exhibit smooth surfaces and larger grain sizes. Furthermore, higher substrate temperatures provide sufficient activation energy and surface mobility for Te atoms, increasing grain size as the atoms occupy suitable positions. Overall, each preparation method has advantages and disadvantages, and a rational choice of method not only meets the needs but also yields specific Te nanostructures for target applications[58–67].

4. Device application

In this section, we will summarize the relevant and emerging applications of elemental Te material. Due to its unique helical structure and remarkable environmental stability, Te is promising to be used in semiconductors and other related fields. This section will introduce the large-scale applications of elemental Te in recent representative devices such as field-effect transistors, photodetectors, and energy harvesting devices.

4.1. Photodetectors

Photodetectors (PDs) are devices that can convert optical signals into electrical signals and are extensively used in optical communications, imaging, and spectral analysis[68, 69]. Elemental Te devices possess excellent properties, including high light absorption, unique structural characteristics, and environmental stability. These attributes make them highly promising for large-scale applications in the field of photodetection, which offer opportunities for advancements in Te-based photodetection technology. The working mechanism of PD includes the following aspects. 1) Light absorption: Pho-

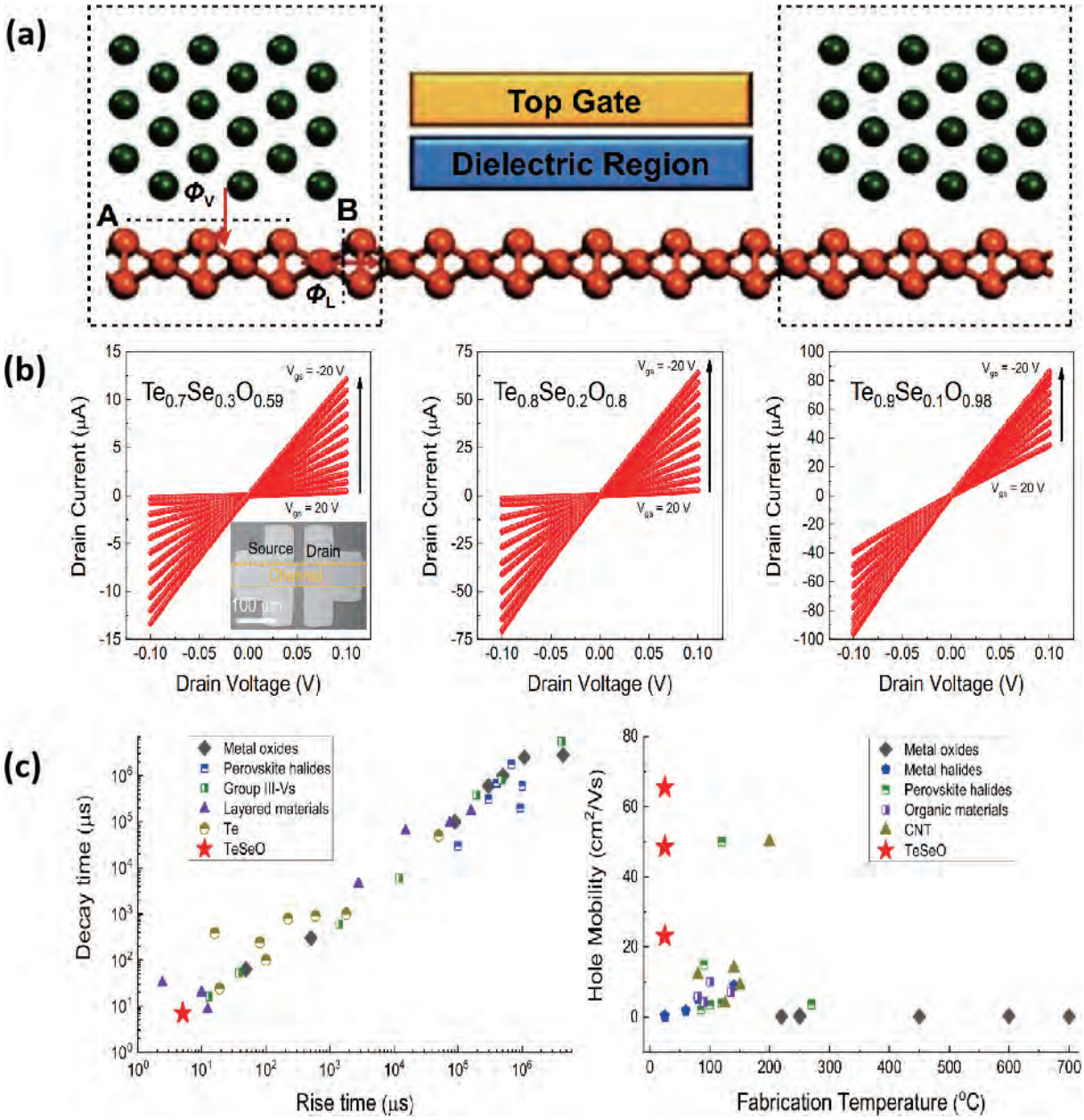

Fig. 7. (Color online) The schematic image and device performance of Te-based FET. (a) Schematic diagram of FETs device based on 2D Te. Adapted permission with Ref. [77], Copyright 2018, Royal Society of Chemistry. (b) The electrical performance of TeSeO FET with different compositions. (c) Comparing the device stability and hole mobility with other traditional materials. Adapted permission with Ref. [81]. Copyright 2024, Nature Publishing Group.

todetectors are designed to absorb incident photons, requiring materials with suitable light absorption properties. While elemental Te devices have a better response to near-infrared light, their performance in detecting visible light is not as good. 2) Carrier generation: When photons are absorbed, their energy excites electron–hole pairs in the material, generating free electron and hole carriers. 3) Carrier separation: Through the influence of a bias or built-in electric field, the electron–hole pairs are separated, forming a photogenerated current. 4) Current amplification: The photogenerated current is then amplified through a series of working principles, including photoconductive, photovoltaic, and photoelectric effects[70–72].

After that, the device characteristics can be characterized to evaluate its performance. Parameters such as detectivity, spectral response range, response time, external quantum efficiency, photocurrent/voltage, and noise effects could be measured[74, 75]. Fig. 6 shows the schematic diagram of quasi-2D Te-based photodetectors under different light wavelengths. The rise and fall times of 52 and 78 μs were obtained at 2.3 μm infrared wavelength, respectively[73]. Te exhibits fast and robust photoresponse, high light absorption, and efficient photocurrent generation in the infrared spectrum. Recently, Dai *et al.*[30] introduced a long-wave infrared polarization-sensitive PTE detectors, utilizing Te as the channel. The PTE effect encompasses two distinct processes: photothermal conversion and the seebeck effect. When a material is exposed to light, the absorbed energy is converted into heat, leading to a localized temperature increase. This temperature rise induces changes in the electronic band structure of the material, consequently altering its electrical properties. Such variations in electrical properties, resulting from tempera-

Table 2. Te nanostructures fabricated by different methods and the main advantages.

Methods	Main nanostructures	Main advantages
Physical vapor deposition[46]	Nanowires and nanoflakes	Well controllability
Chemical vapor deposition[16]	Nanowires and nanoflakes	Controlled reaction conditions
Van der Waals epitaxy[49]	2D layered structures	Heterogeneous integration
Hydrothermal[58, 59, 54]	Nanowires and nanonet	High throughput
Thermal evaporation[60, 57, 61]	Thin film	Uniform deposition
Liquid phase exfoliation[62–67]	2D layered structures	High efficiency

Table 3. Comparison of different nanomaterials used in FET.

Materials	On/off current ratio	Responsibility	Mobility ($cm^2/(V·s)$)
Te nanoflakes[52]	10^5	13 A/W	700
Te thin film[19]	10^4	–	35
$MoTe_2$[82]	10^6	–	27
Black phosphorus[78, 83]	10^5	4.8 mA/W	1000
MoS_2[84, 85]	–	5.2 A/W	120
WS_2[86, 87]	–	21.2 μA/W	140
WSe_2[88]	–	0.92 A/W	142

ture fluctuations, offer a potent platform for optoelectronic detection. This platform enables the transmission of optical signals to electrical readout, independent of the bandgap of the active material. Besides, Guo *et al.*[76] prepared elemental Te film by sputtering, based on the seebeck effect as well as high seebeck coefficient ~312 μ·V·K^{-1}, and found that the Te film device can be used for the temperature warning function of electronic skin. The researchers designed and prepared a flexible infrared PTE detector that senses thermal radiation from surrounding objects and converts it into an electrical signal. By integrating the detector into an electronic skin, real-time monitoring and early warning of temperature changes can be realized. This research provides new ideas and methods for the application of electronic skin in health monitoring, human-computer interaction, and smart equipment.

4.2. Field-effect transistor

Field-effect transistor is an essential electronic device with three terminals: source, drain, and gate while a schematic picture of a Te-based FET can be found in Fig. 7(a)[77]. Its operation relies on controlling the current flow between the source and drain by applying a gate voltage. The performance of FETs is primarily assessed based on their switching characteristics, including field-effect mobility, on/off current ratio, threshold voltage, switching speed, and operation stability.

Recently, there has been a growing demand for inorganic p-type semiconductors with high hole mobility and ambient stability. While several n-type semiconductors have been successfully developed, progress in developing p-type counterparts has been limited. Only certain inorganic materials have demonstrated exceptional performance in p-channel FETs. For example, Li *et al.*[78] and Du *et al.*[79] reported the first FET based on 2D black phosphorus material, in which the field effect hole mobility is 1000 $cm^2/(V·s)$, and the on/off current ratio can be greater than 10^5, which is substantially better than TMDCs-based p-type devices. However, as we mentioned in Table 1, the BP devices have poor ambient stability, so the instability problem prevents them from being used on a large-scale practical application. Zhao *et al.*[4] reported the realization of elemental Te thin film by low-temperature thermal evaporation for manufacturing high-performance wafer-scale p-type field-effect transistors. According to the experiment data, the mobility can reach roughly 35 $cm^2/(V·s)$ with an on/off current ratio of ~10^4 on an 8 nm-thick Te film.

Besides, Wang *et al.*[59] have reported a higher performance FET based on 2D Te nanoflakes synthesized by hydrothermal synthesis. The fabricated device showed an on/off current ratio of approximately 10^5. Moreover, field-effect hole mobility of roughly 700 $cm^2/(V·s)$ was achieved for the optimum thickness of roughly 15 nm. Compared with the devices based on polycrystalline Te thin film prepared by Zhao *et al.*[4], crystalline 2D Te nanostructures have a better performance when used in FET. In addition, they confirm that the device stored in ambient condition for one month does not cause device failure even with no surface passivation. This reliable device stability of Te promises the development of inorganic p-channel FETs. In Table 3, the FET performance based on different materials has been summarized[82–88].

Most recently, Liu *et al.*[80] developed the thin-film transistors based on p-type Se-alloyed Te–TeO_x ($0 < x \leqslant 2$) film. Due to the incorporation of Se alloying into Te-based devices, hole concentration is effectively suppressed, and p-orbital overlap is promoted, resulting in high hole mobility FETs which can achieve hole mobility 15 $cm^2/(V·s)$ and the on/off current ratio of 10^6 to 10^7. Both wafer-scale uniformity and long-term environmental stability under bias stress were demonstrated in this work. In the meantime, Meng *et al.*[81] discovered the p-channel inorganic semiconductor compound tellurium-selenium-oxygen (TeSeO). The compound also showed some intrinsic p-channel properties of Te with a tunable bandgap of 0.7–2.2 eV. TeSeO devices showed a high hole mobility of 48.5 $cm^2/(V·s)$, a high responsibility of 603 A/W, and an ultrafast response of 5 μs. In Figs. 7(b) and 7(c), TeSeO devices perform better than their counterparts in FET and PD. This suggests that while BP may have better hole mobility, the Te-based material may outperform in terms of on/off ratio, response time, and stability.

4.3. Gas sensor

Gas sensors play a crucial role in detecting and identifying the composition and concentration of gases. They convert this information into electrical signals for analysis and processing, finding applications in environmental monitoring and other fields[89, 90]. As environmental awareness grows, gas sensors have made significant improvements in performance, reliability, and cost. This section specifically focuses on using Te-based semiconductors in gas sensing applications to differentiate various gases.

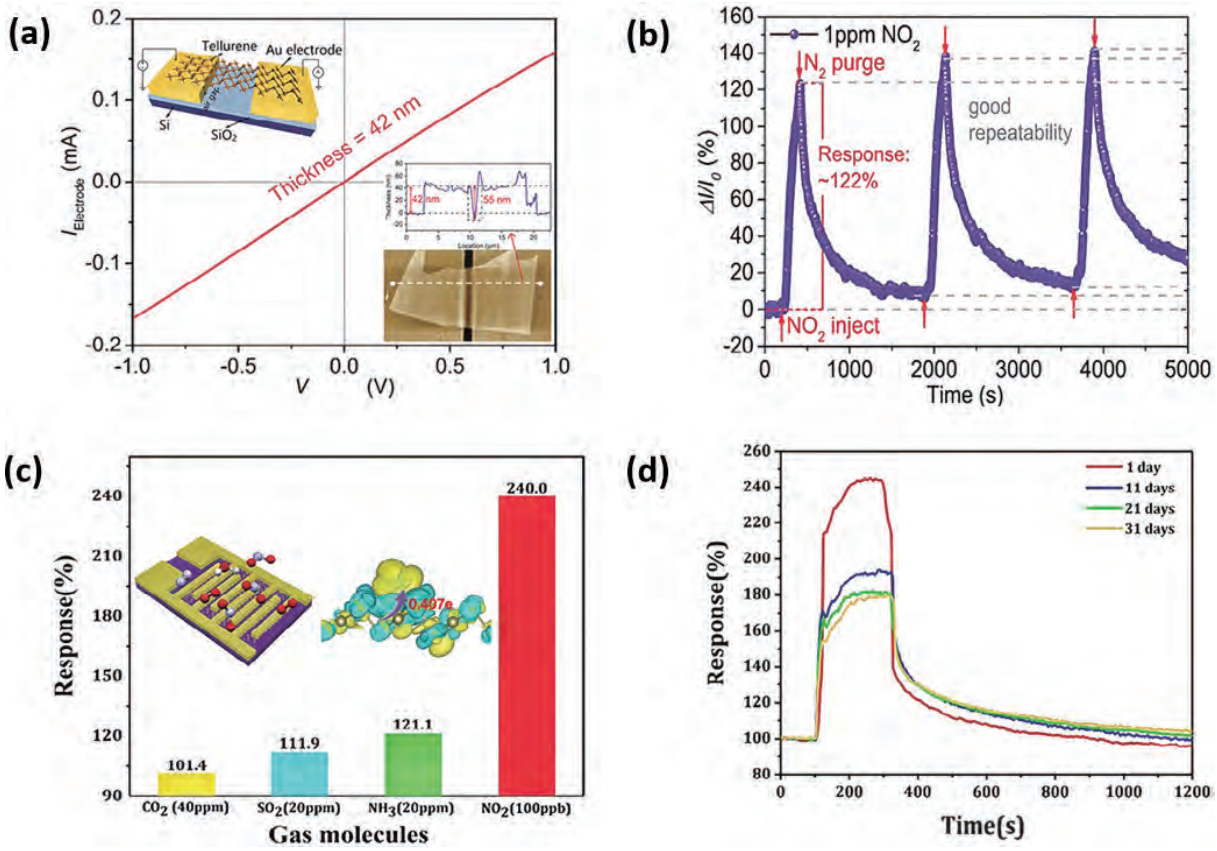

Fig. 8. (Color online) The testing results of gas sensors enabled by elemental Te. (a) The *I*–*V* curve of 42 nm Te devices. Inset top: The schematic diagram of Te-based device. Inset bottom: The AFM characterization image of Te nanoflake. (b) Current response of NO_2. Adapted permission with Ref. [94]. Copyright 2019, The Royal Society of Chemistry. (c) NO_2 selectivity of a Te gas sensor. Inset: The schematic diagrams of detection. (d) The environmental stability of Te-based devices. Adapted permission with Ref. [95]. Copyright 2020, The American Chemical Society.

In 2001, Tsiulyanu *et al.* reported the spiral structure of Te alloys, also indicating their potential for use in gas sensors. These Te-based sensors have the ability to detect various gases, with the highest sensitivity being towards nitrogen dioxide[56]. Such outstanding sensitivity results from the interaction between nitrogen oxides and Te alloys, which enhances the device's ability to adsorb oxygen, increasing hole concentration and conductivity within the material. Nitrogen dioxide is recognized as one of the six major gaseous pollutants worldwide, highlighting the importance of utilizing Te alloys for nitrogen dioxide sensing. However, in the case of Te thin film, Sen *et al.* discovered that when these films were used as toxic gas sensors, their resistance would increase reversely when exposed to reducing gases. In contrast, the opposite effect was observed when exposed to oxidizing gases[91]. In another work, the gas sensitivity of these films to gases such as NH_3, H_2S, and NO_2 was measured to be shifted at different temperatures. Specifically, the sensitivity of Te film gases decreased with increasing temperature, with a significant decrease in sensitivity (<10%) for all gases at T ~ 373 K.

Also, it has been found that the gas-sensitive properties of these Te thin films are significantly affected during processing and preparation. For instance, high substrate temperatures and annealing conditions will lead to degradation of the device performance, even though there is no difference in the morphology. Tsiulyanu *et al.*[56] experimentally demonstrated that the gas sensitivity of elemental Te membranes to NO_2 is strongly dependent on the thickness of the membrane. In addition, the performance will be drastically reduced when the preparation or device temperature is higher than 373 K. Meanwhile, Bhandarkar *et al.*[92] investigated the sensitivity of external factors, such as different substrates and different synthesis temperatures, to the representative gas NO_2 based on the consistency of the Te film thickness.

The p-type conductance in elemental Te arises from the presence of crystal defects that lead to the formation of additional receptor centers[93]. The excess charge generated when the elemental Te device interacts with the gas is trapped in the defect centers, resulting in reduced conductivity. On the other hand, adsorbed oxygen could also capture electrons and form TeO_2 by chemisorption, which leads to the transfer of surface charges and the bending of energy bands in Te semiconductors. In this regard, exposure to reducing gases such as H_2S or NH_3 reduces the hole concentration and thus increases the film resistivity. When exposed to oxidizing gases such as NO_2, enhanced oxidation at the film surface results in the increase of hole concentration and the decrease of film resistivity. Recently, Wang *et al.*[94] reported a gas sensor based on elemental Te devices. These devices exhibit high sensitivity and selectivity towards various gases, such as a large detection range (from 25 ppb to 5 ppm) and low baseline noise (~0.5%). Through density functional theory calculations, it is proposed that the large adsorption energy and strong charge redistribution endow Te has high sensitivity and selectivity for NO_2 detection. In Figs. 8(a) and 8(b), excellent conductivity and NO_2 sensitivity were demonstrated on 42 nm thick Te nanoflakes. In addition, Cui *et al.*[95] found

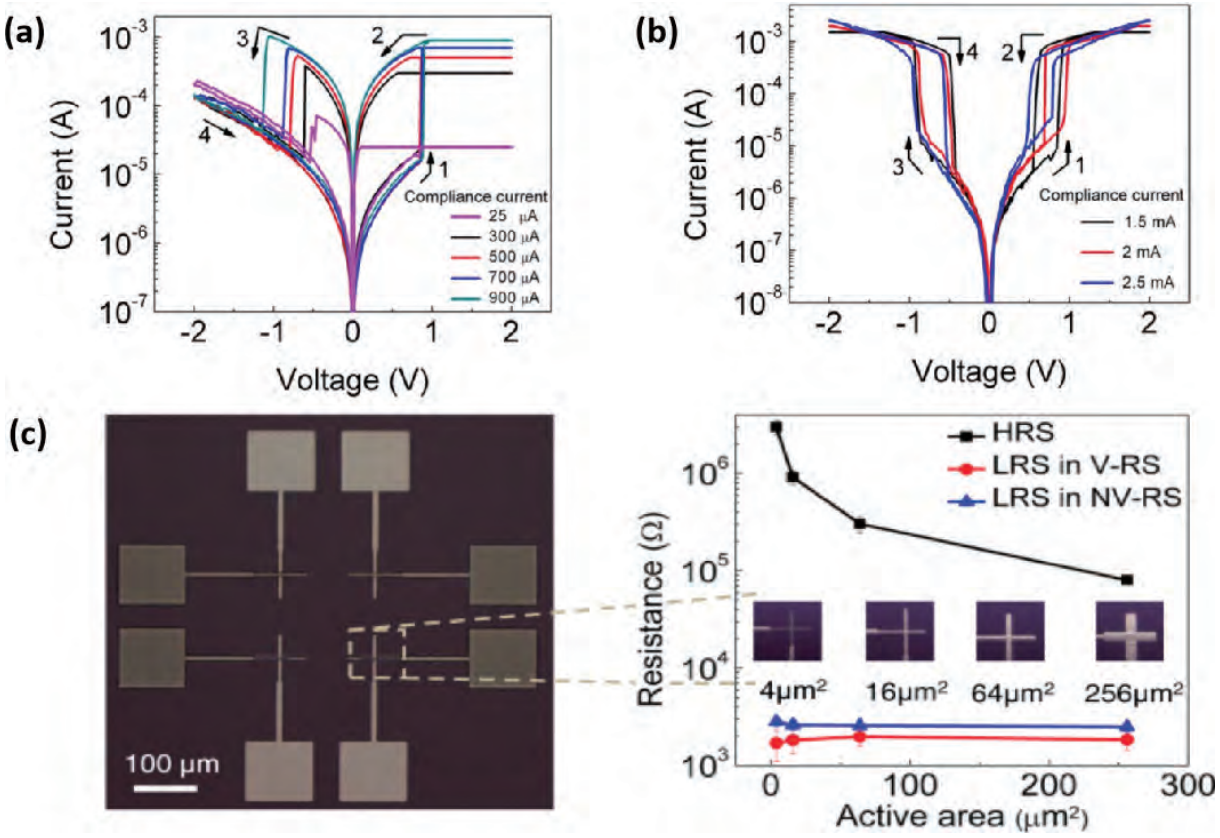

Fig. 9. (Color online) The resistive switching device based on elemental Te. (a), (b) Nonlinear *I*–*V* relationship of Te device in NV-RS and V-RS modes. (c) The device schematic diagram and device resistance as a function of the active area. Adapted permission with Ref. [98]. Copyright 2021, Nature Publishing Group.

that Te nanosheets have high selectivity and sensitivity (25 ppb/83 s and 100 ppb/26 s) towards NO_2 gas, can reach a sub-ppb detection limit, and have long-term stability for over one month.

4.4. Resistive switching devices

With the rapid growth of information in the era of big data, there is a need to overcome the declining cost-effectiveness of device scaling through new building blocks[96, 97]. Resistive switcher (RS) is a common electronic component mainly used to regulate the voltage or current in a circuit. It consists of two components: volatile selector and nonvolatile memory, with different operating current requirements.

Yang *et al.* [98] reported the resistive switching devices based on the elemental Te filaments, which can act as a selector or a memory in the respective desired current range, highlighting the important application prospects in advancing memory and computing technologies. It is demonstrated that single Te-based devices can be used for different functions. For large-scale one-selector and one-resistor (1S1R) cross-point arrays, NV-RS (memory device) and V-RS (selector device) are two induvial parts of array configurations, with the former focusing on nonvolatile data storage and the latter on volatile data selection. In Fig. 9, it can be seen that the compliance current in V-RS mode is one order of magnitude higher than NV-RS. Notably, the anomalous long-term plasticity (LTP) to short-term plasticity (STP) transition observed in this work also proves that the elemental Te-based devices have the potential to be rectifiers in analog computers. In addition, Sahu *et al.*[99] discovered that the Ag/TiO_2/FTO devices, modulated by the magnetic field, possess bipolar resistive switching. Given the Lorentz force and doping effect, the device alters voltage to perform a switching function. Before, the resistive switching has been established in devices with doped magnetic components[100, 101]. This work breaks the traditional rule where voltage is the only factor that can control the transport and switching characteristics, by which the magnetic field is added to regulate the resistive switching of Te material. The RS effect is mainly based on binary transition metal oxides[102–104] such as NiO, ZnO, and TiO_2. At the same time, the elemental Te device displayed a faster response time with improved current accuracy on both negative and positive sides.

4.5. Energy harvesting device

With the gradual depletion of non-renewable resources and the increasing environmental problems, the energy crisis has become a pressing issue[105–107]. For developing renewable and environmental friendly energy sources, attention has been paid to collecting waste heat from relevant plants. Elemental Te is a material with high energy-efficiency thermoelectricity. As mentioned before, the unique thermoelectric effect and stability allow it to become the next generation of thermoelectric collection devices.

Based on the seebeck effect, the temperature gradient between the two terminals of the device could generate an output signal. This allows the conversion of heat-induced temperature effects into a more easily measurable current magnitude[108]. Notably, it can be observed that as the temperature difference improves, both the thermoelectric current and volt-

age increase simultaneously. Additionally, solar energy can also be utilized by irradiating a specific area and efficiently converting it into electrical energy using the PTE effect. Recently, Wu *et al.*[109] using first-principles DFT simulations, the maximum power conversion efficiency of the Te/WTe_2 and $Te/MoTe_2$ heterojunction solar cells was calculated to be 22.5% and 20.1%, respectively. Also, the thermoelectric performance (i.e., ZT value) of elemental Te (0.63)[109] is larger than that of graphene (0.42)[110], black phosphorus (0.25)[111], and organometallic perovskite $CH_3NH_3PbI_3$ (0.13)[112].

5. Conclusion

After nearly 250 years of discovering elemental Te in 1782, it has become an important industrial raw and high-tech material. In this paper, we reviewed the synthesis pathways of Te nanostructures and the applications of elemental Te in various fields, such as photodetectors, PTE detectors, FETs, gas sensors, etc., which have gained intense attention in recent years. As a representative material of new p-type semiconductors, Te exhibits outstanding hole mobility of ~10^3 $cm^2/(V{\cdot}s)$ at room temperature and a tunable bandgap ranging from 0.35 to 1.2 eV, as well as structural anisotropy compared to conventional inorganic p-type semiconductors. Additionally, its environmental and device operating stability outperforms most p-type inorganic materials. There is no composition control issue for single-element Te, making it easier to prepare and not requiring strict control of stoichiometric ratios. In recent decades, Te has gained significant attention due to its exceptional and versatile performance, aiming to apply Te to meet diverse application requirements and drive the rapid advancement of the semiconductor industry.

Although elemental Te nanostructures offer enormous potential for academic and engineering applications, challenges and opportunities still remain. For the synthesis process, elemental Te nanostructures with different shapes and orientations can be synthesized by PVD, CVD, etc. However, the growth chamber typically needs high growth temperature, low growth pressure, and a vacuum environment. Thus, versatile Te synthesis methods should be found to solve the strict growth requirements and the cost-effectiveness issue. Moreover, several nanostructured synthesis methods have been widely used to synthesize few-layer materials that are also highly efficient, such as vapor deposition and solution deposition. However, few synthesis methods have been reported to be able to produce large-scale ultrathin Te materials. Therefore, it is crucial to discover techniques for controllable production synthesis to grow Te with the required number of layers from monolayer to multilayer.

As for devices and applications, recent studies on elemental Te PDs are mostly focused on the visible and infrared regions. Devices suitable for ultra-wideband photodetection are the priority and should also be considered in future studies. Additionally, the transport mechanisms of elemental Te are not well understood compared to black phosphorus and transition metal dichalcogenides, while the development of the doping technique and heterojunction formation process are still in the primary stage[113]. Therefore, to further enhance the performance of Te-based devices, it is necessary to improve doping and heterojunction fabrication techniques[114, 115]. Besides, because elemental Te is susceptible to oxidation in air, it is required to prove by XPS that it is the elemental Te responsible for the properties and not the telluride.

Additionally, only a few articles have reported on high-performance semiconductor materials for neuromorphic devices based on Te. Thus, more studies are needed to simulate the structure and function of the biological nervous system. Given the high mobility and high sensitivity of Te, further progress on Te-based neuromorphic devices can provide a way to help solve the energy dissipation problem[113]. Furthermore, there is a lack of integration and compatibility when using elemental Te in resistive switching applications. Further investigations should not be limited to the storage area, with an equal focus on the in-sensor-computing and near-sensor-computing areas would be ideal. Enabled by the circularly polarized light (CPL) coupling, Te-based materials can be used to develop components for CPL optical communication systems, potentially increasing data transmission rates and improving signal integrity. Liu *et al.*[116] proposed to integrate CPL sensitivity with optical learning and memory in a photonic artificial synapse (PAS) device, which can achieve up to 93% recognition accuracy in spiking neural network simulations. Notably, helical Te chains align along the *c*-axis, which fulfills the requirement of designing efficient and stable CPL light devices, and further research is necessary for functional optoelectronic utilizations. Besides the applications mentioned above, elemental Te has many promising utilization opportunities, such as flexible electronics, display electronics, integrated chips, and biomedicine technology.

Acknowledgments

This work is supported by a fellowship award from the Research Grants Council of the Hong Kong Special Administrative Region, China (CityU RFS2021−1S04) and the Innovation and Technology Fund (MHP/044/23) from the Innovation and Technology Commission of the Hong Kong Government Special Administrative Region, China.

References

[1] Shi Z, Cao R, Khan K, et al. Two-dimensional tellurium: progress, challenges, and prospects. Nano-Micro Lett, 2020, 12(1), 99

[2] Tang B, Sun L, Zheng W, et al. Ultrahigh quality upconverted single-mode lasing in cesium lead bromide spherical microcavity. Adv Opt Mater, 2018, 6(20), 1800391

[3] Yin Y, Cao R, Guo J, et al. High-speed and high-responsivity hybrid silicon/black-phosphorus waveguide photodetectors at 2 μm. Laser & Photonics Rev, 2019, 13(6), 1900032

[4] Zhao C, Tan C, Lien D-H, et al. Evaporated tellurium thin films for p-type field-effect transistors and circuits. Nat Nanotechnol, 2020, 15(1), 53

[5] Zhou G, Addou R, Wang Q, et al. High-mobility helical tellurium field-effect transistors enabled by transfer-free, low-temperature direct growth. Adv Mater, 2018, 30(36), 1803109

[6] Ba L A, Döring M, Jamier V, et al. Tellurium: an element with great biological potency and potential. Org & Biomol Chem, 2010, 8(19), 4203

[7] Liu J W, Zhu J H, Zhang C L, et al. Mesostructured assemblies of ultrathin superlong tellurium nanowires and their photoconductivity. J Am Chem Soc, 2010, 132(26), 8945

[8] Peng H, Kioussis N, Snyder G J. Elemental tellurium as a chiral p-type thermoelectric material. Phys Rev B, 2014, 89(19), 195206

[9] Hermann J P, Quentin G, Thuillier J M. Determination of the d_{14} piezoelectric coefficient of tellurium. Solid State Commun, 1969, 7(1), 161

[10] Liu A, Zhu H, Zou T, et al. Evaporated nanometer chalcogenide films for scalable high-performance complementary electronics. Nat Commun, 2022, 13(1), 6372

[11] Zha J, Dong D, Huang H, et al. Electronics and optoelectronics based on tellurium. Adv Mater, 2024, 36 (45), 2408969

[12] Furukawa T, Shimokawa Y, Kobayashi K, et al. Observation of current-induced bulk magnetization in elemental tellurium. Nat Commun, 2017, 8(1), 954

[13] Cheng B, Gao Y, Zheng Z, et al. Giant nonlinear Hall and wireless rectification effects at room temperature in the elemental semiconductor tellurium. Nat Commun, 2024, 15(1), 5513

[14] Zhu Z, Cai X, Yi S, et al. Multivalency-driven formation of te-based monolayer materials: A combined first-principles and experimental study. Phys Rev Lett, 2017, 119(10), 106101

[15] Yan C W, Zhou L, Guo P, et al. Two ultra-stable novel allotropes of tellurium few-layers. Chin Phys B, 2020, 29(9), 97103

[16] Meng Y, Li X, Kang X, et al. Van der Waals nanomesh electronics on arbitrary surfaces. Nat Commun, 2023, 14(1), 2431

[17] Qiao J, Pan Y, Yang F, et al. Few-layer tellurium: one-dimensional-like layered elementary semiconductor with striking physical properties. Sci Bull, 2018, 63(3), 159

[18] Sang D K, Wen B, Gao S, et al. Electronic and optical properties of two-dimensional tellurene: from first-principles calculations. Nanomater, 2019, 9(8), 1075

[19] Qiu G, Charnas A R, Niu C, et al. The resurrection of tellurium as an elemental two-dimensional semiconductor. npj 2D Mater Appl, 2022, 6(1), 17

[20] Xian L, Pérez Paz A, Bianco E, et al. Square selenene and tellurene: novel group VI elemental 2D materials with nontrivial topological properties. 2D Mater, 2017, 4(4), 041003

[21] Peng B, Zhang H, Shao H, et al. The electronic, optical, and thermodynamic properties of borophene from first-principles calculations. J Mater Chem C, 2016, 4(16), 3592

[22] Kuang Y D, Lindsay L, Shi S Q, et al. Tensile strains give rise to strong size effects for thermal conductivities of silicene, germanene and stanene. Nanoscale, 2016, 8(6), 3760

[23] Yang K, Cahangirov S, Cantarero A, et al. Thermoelectric properties of atomically thin silicene and germanene nanostructures. Phys Rev B, 2014, 89(12), 125403

[24] Zheng J, Chi F, Guo Y. Exchange and electric fields enhanced spin thermoelectric performance of germanene nano-ribbon. J Phys Condens Matter, 2015, 27(29), 295302

[25] Gao Z, Tao F, Ren J. Unusually low thermal conductivity of atomically thin 2D tellurium. Nanoscale, 2018, 10(27), 12997

[26] Lin S, Li W, Zhang X, et al. Sb induces both doping and precipitation for improving the thermoelectric performance of elemental Te. Inorg Chem Front, 2017, 4(6), 1066

[27] An D, Zhang S, Zhai X, et al. Metavalently bonded tellurides: the essence of improved thermoelectric performance in elemental Te. Nat Commun, 2024, 15(1), 3177

[28] Zhang M, Liu Y, Guo F, et al. High-performance flexible broadband photothermoelectric photodetectors based on tellurium films. ACS Appl Mater Interfaces, 2024, 16(5), 6152

[29] Huang J, You C, Wu B, et al. Enhanced photothermoelectric conversion in self-rolled tellurium photodetector with geometry-induced energy localization. Light: Sci Appl, 2024, 13(1), 153

[30] Dai M, Wang C, Qiang B, et al. On-chip mid-infrared photothermoelectric detectors for full-Stokes detection. Nat Commun, 2022, 13(1), 4560

[31] Zhang Y, Meng Y, Wang L, et al. Pulse irradiation synthesis of metal chalcogenides on flexible substrates for enhanced photothermoelectric performance. Nat Commun, 2024, 15(1), 728

[32] Budania P, Baine P, Montgomery J, et al. Long-term stability of mechanically exfoliated MoS_2 flakes. MRS Commun, 2017, 7(4), 813

[33] Liu L, Tang J, Wang Q Q, et al. Thermal stability of MoS_2 encapsulated by graphene. Acta Phys Sin, 2018, 67(22), 226501

[34] Liu Y C, Wang V, Xia M G, et al. First-principles study on structural, thermal, mechanical and dynamic stability of T′-MoS_2. J Phys: Condens Matter, 2017, 29(9), 095702

[35] Yang H, Zhang Y, Hu F, et al. Urchin-like CoP nanocrystals as hydrogen evolution reaction and oxygen reduction reaction dual-electrocatalyst with superior stability. Nano Lett, 2015, 15(11), 7616

[36] Zhao C, Hurtado L, Javey A. Thermal stability for Te-based devices. Appl Phys Lett, 2020, 117(19), 192104

[37] Hong Y, Zhang J, Zeng X C. Thermal contact resistance across a linear heterojunction within a hybrid graphene/hexagonal boron nitride sheet. Phys Chem Chem Phys, 2016, 18(35), 24164

[38] Lim D, Kannan E S, Lee I, et al. High performance MoS_2-based field-effect transistor enabled by hydrazine doping. Nanotechnol, 2016, 27(22), 225201

[39] Xu Y, Shi Z, Shi X, et al. Recent progress in black phosphorus and black-phosphorus-analogue materials: properties, synthesis and applications. Nanoscale, 2019, 11(31), 14491

[40] Iqbal M W, Iqbal M Z, Khan M F, et al. High-mobility and air-stable single-layer WS_2 field-effect transistors sandwiched between chemical vapor deposition-grown hexagonal BN films. Sci Rep, 2015, 5(1), 10699

[41] Khalil H M W, Khan M F, Eom J, et al. Highly stable and tunable chemical doping of multilayer WS_2 field effect transistor: Reduction in contact resistance. ACS Appl Mater Interfaces, 2015, 7(42), 23589

[42] Huang H H, Fan X, Singh D J, et al. Recent progress of TMD nanomaterials: phase transitions and applications. Nanoscale, 2020, 12(3), 1247

[43] Zhang Y, Yao Y, Sendeku M G, et al. Recent progress in CVD growth of 2D transition metal dichalcogenides and related heterostructures. Adv Mater, 2019, 31(41), e1901694

[44] Hong S, Im H, Hong Y K, et al. N-type doping rffect of CVD-grown multilayer $MoSe_2$ thin film transistors by two-step functionalization. Adv Electro Mater, 2018, 4(12), 1800308

[45] Larentis S, Fallahazad B, Tutuc E. Field-effect transistors and intrinsic mobility in ultra-thin $MoSe_2$ layers. Appl Phys Lett, 2012, 101, 223104

[46] Apte A, Bianco E, Krishnamoorthy A, et al. Polytypism in ultrathin tellurium. 2D Mater, 2019, 6(1), 015013

[47] Métraux C, Grobety B. Tellurium nanotubes and nanorods synthesized by physical vapor deposition. J Mater Res, 2004, 192159

[48] Xu M, Xu J, Luo L, et al. Hydrogen-assisted growth of one-dimensional tellurium nanoribbons with unprecedented high mobility. Materials Today, 2023, 6350

[49] Wang Q, Safdar M, Xu K, et al. Van der Waals epitaxy and photoresponse of hexagonal tellurium nanoplates on flexible mica sheets. ACS Nano, 2014, 8(7), 7497

[50] Li D, Meng Y, Zhang Y, et al. Selective surface engineering of perovskite microwire arrays. Adv Funct Mater, 2023, 33(33), 2302866

[51] Cheng R, Wen Y, Yin L, et al. Ultrathin single-crystalline CdTe nanosheets realized via van der Waals epitaxy. Adv Mater, 2017, 29(35), 1703122

[52] Xie Z, Xing C, Huang W, et al. Ultrathin 2D nonlayered tellurium nanosheets: Facile liquid-phase exfoliation, characterization, and photoresponse with high performance and enhanced stability. Adv Funct Mater, 2018, 28(16), 1705833

[53] Ben-Moshe A, Wolf S G, Sadan M B, et al. Enantioselective control of lattice and shape chirality in inorganic nanostructures us-

ing chiral biomolecules. Nat Commun, 2014, 5(1), 4302
[54] Naqi M, Choi K H, Yoo H, et al. Nanonet: Low-temperature-processed tellurium nanowire network for scalable p-type field-effect transistors and a highly sensitive phototransistor array. NPG Asia Mater, 2021, 13(1), 46
[55] Mo M, Zeng J, Liu X, et al. Controlled hydrothermal synthesis of thin single-crystal tellurium nanobelts and nanotubes. Adv Mater, 2002, 14(22), 1658
[56] Tsiulyanu D, Marian S, Miron V, et al. High sensitive tellurium based NO_2 gas sensor. Sens Actuators B: Chem, 2001, 73(1), 35
[57] Okuyama K, Kumagai Y. Grain growth of evaporated Te films on a heated and cooled substrate. J Appl Phys, 1975, 46(4), 1473
[58] Amani M, Tan C, Zhang G, et al. Solution-synthesized high-mobility tellurium nanoflakes for short-wave infrared photodetectors. ACS Nano, 2018, 12(7), 7253
[59] Fang Q, Shang Q, Zhao L, et al. Ultrafast charge transfer in perovskite nanowire/2d transition metal dichalcogenide heterostructures. J Phys Chem Lett, 2018, 9(7), 1655
[60] Dutton R W, Muller R S. Electrical properties of tellurium thin films. Proc IEEE, 1971, 59(10), 1511
[61] Weimer P K. A p-type tellurium thin-film transistor. Proceedings of the IEEE, 1964, 52(5), 608
[62] Ge Y, Chen S, Xu Y, et al. Few-layer selenium-doped black phosphorus: synthesis, nonlinear optical properties and ultrafast photonics applications. J Mater Chem C, 2017, 5(25), 6129
[63] Guo Z, Zhang H, Lu S, et al. From black phosphorus to phosphorene: basic solvent exfoliation, evolution of raman scattering, and applications to ultrafast photonics. Adv Funct Mater, 2015, 25(45), 6996
[64] Huang W, Xing C, Wang Y, et al. Facile fabrication and characterization of two-dimensional bismuth(iii) sulfide nanosheets for high-performance photodetector applications under ambient conditions. Nanoscale, 2018, 10(5), 2404
[65] Li J, Luo H, Zhai B, et al. Black phosphorus: a two-dimension saturable absorption material for mid-infrared Q-switched and mode-locked fiber lasers. Sci Rep, 2016, 6(1), 30361
[66] Wu W, Qiu G, Wang Y, et al. Tellurene: its physical properties, scalable nanomanufacturing, and device applications. Chem Soc Rev, 2018, 47(19), 7203
[67] Xu Y, Wang Z, Guo Z, et al. Solvothermal synthesis and ultrafast photonics of black phosphorus quantum dots. Adv Opt Mater, 2016, 4(8), 1223
[68] Hu C, Chai R, Wei Z, et al. ZnSb/Ti_3C_2Tx MXene van der Waals heterojunction for flexible near-infrared photodetector arrays. J Semicond, 2024, 45(5), 052601
[69] Long Z, Ding Y, Qiu X, et al. A dual-mode image sensor using an all-inorganic perovskite nanowire array for standard and neuromorphic imaging. J Semicond, 2023, 44(9), 092604
[70] Koppens F H L, Mueller T, Avouris P, et al. Photodetectors based on graphene, other two-dimensional materials and hybrid systems. Nat Nanotechnol, 2014, 9(10), 780
[71] Long M, Wang P, Fang H, et al. Progress, challenges, and opportunities for 2D material based photodetectors. Adv Funct Mater, 2019, 29(19), 1803807
[72] Sun Z, Chang H. Graphene and graphene-like two-dimensional materials in photodetection: mechanisms and methodology. ACS Nano, 2014, 8(5), 4133
[73] Tong L, Huang X, Wang P, et al. Stable mid-infrared polarization imaging based on quasi-2D tellurium at room temperature. Nat Commun, 2020, 11(1), 2308
[74] Li X, Meng Y, Li W, et al. Multislip-enabled morphing of all-inorganic perovskites. Nat Mater, 2023, 22(10), 1175
[75] Meng Y, Zhang Y, Lai Z, et al. Au-seeded $CsPbI_3$ nanowire optoelectronics via exothermic nucleation. Nano Lett, 2023, 23(3), 812
[76] Guo X, Lu X, Jiang P, et al. Touchless thermosensation enabled by flexible infrared photothermoelectric detector for temperature prewarning function of electronic skin. Adv Mater, 2024, 36(23), e2313911
[77] Yan J, Zhang X, Pan Y, et al. Monolayer tellurene–metal contacts. J Mater Chem C, 2018, 6(23), 6153
[78] Li L, Yu Y, Ye G J, et al. Black phosphorus field-effect transistors. Nat Nanotechnol, 2014, 9(5), 372
[79] Du Y, Maassen J, Wu W, et al. Auxetic black phosphorus: A 2D material with negative poisson's ratio. Nano Lett, 2016, 16(10), 6701
[80] Liu A, Kim Y S, Kim M G, et al. Selenium-alloyed tellurium oxide for amorphous p-channel transistors. Nature, 2024, 629(8013), 798
[81] Meng Y, Wang W, Fan R, et al. An inorganic-blended p-type semiconductor with robust electrical and mechanical properties. Nat Commun, 2024, 15(1), 4440
[82] Pradhan N R, Rhodes D, Feng S, et al. Field-effect transistors based on few-layered α-$MoTe_2$. ACS Nano, 2014, 8(6), 5911
[83] Liu X, Qu D, Li H M, et al. Modulation of quantum tunneling via a vertical two-dimensional black phosphorus and molybdenum disulfide p-n junction. ACS Nano, 2017, 11(9), 9143
[84] Lee J, Mak K F, Shan J. Electrical control of the valley Hall effect in bilayer MoS_2 transistors. Nat Nanotechnol, 2016, 11(5), 421
[85] Wang W, Klots A, Prasai D, et al. Hot electron-based near-infrared photodetection using bilayer MoS_2. Nano Lett, 2015, 15(11), 7440
[86] Movva H C P, Rai A, Kang S, et al. High-mobility holes in dual-gated WSe_2 field-effect transistors. ACS Nano, 2015, 9(10), 10402
[87] Perea-López N, Elías A L, Berkdemir A, et al. Sensors: photosensor device based on few-layered WS_2 films. Adv Funct Mater, 2013, 23(44), 5510
[88] Yang T, Zheng B, Wang Z, et al. Van der Waals epitaxial growth and optoelectronics of large-scale WSe_2/SnS_2 vertical bilayer p–n junctions. Nat Commun, 2017, 8(1), 1906
[89] Dey A. Semiconductor metal oxide gas sensors: A review. Mater Sci Eng: B, 2018, 229(1), 206
[90] Shendage S S, Patil V L, Vanalakar S A, et al. Sensitive and selective NO_2 gas sensor based on WO_3 nanoplates. Sens Actuators B-chem, 2017, 240(1), 426
[91] Sen S, Bhandarkar V, Muthe K, et al. Chapter 7 Tellurium thin films based gas sensor, science and technology of chemiresistor gas sensors. New York: Nova Science Publishers Inc., 2007
[92] Bhandarkar V, Sen S, Muthe K P, et al. Effect of deposition conditions on the microstructure and gas-sensing characteristics of Te thin films. Mater Sci Eng: B, 2006, 131(1), 156
[93] Capers M, White M L. The electrical properties of vacuum deposited tellurium films. Thin Solid Films, 1973, 15(1), 5
[94] Wang D, Yang A, Lan T, et al. Tellurene based chemical sensor. J Mater Chem A, 2019, 7(46), 26326
[95] Cui H, Zheng K, Xie Z, et al. Tellurene nanoflake-based NO_2 sensors with superior sensitivity and a sub-parts-per-billion detection limit. ACS Appl Mater Interfaces, 2020, 12(42), 47704
[96] Meng Y, Li F, Lan C, et al. Artificial visual systems enabled by quasi-two-dimensional electron gases in oxide superlattice nanowires. Sci Adv, 2020, 6(46), eabc6389
[97] Wang Z, Wu H, Burr G W, et al. Resistive switching materials for information processing. Nat Rev Mater, 2020, 5(3), 173
[98] Yang Y, Xu M, Jia S, et al. A new opportunity for the emerging tellurium semiconductor: making resistive switching devices. Nat Commun, 2021, 12(1), 6081
[99] Sahu D P, Jammalamadaka S N. Remote control of resistive switching in TiO_2 based resistive random access memory device. Sci Rep, 2017, 7(1), 17224

[100] Chen G, Song C, Chen C, et al. Resistive switching and magnetic modulation in cobalt-doped ZnO. Adv Mater, 2012, 24(26), 3515
[101] Krzysteczko P, Reiss G, Thomas A. Memristive switching of MgO based magnetic tunnel junctions. Appl Phys Lett, 2009, 95(11), 112508
[102] Chen C H, Pan F, Wang Z S, et al. Bipolar resistive switching with self-rectifying effects in Al/ZnO/Si structure. J Appl Phys, 2012, 111(1), 013702
[103] Kwon D H, Kim K M, Jang J H, et al. Atomic structure of conducting nanofilaments in TiO_2 resistive switching memory. Nat Nanotechnol, 2010, 5(2), 148
[104] Seo S, Lee M J, Kim D C, et al. Electrode dependence of resistance switching in polycrystalline NiO films. Appl Phys Lett, 2005, 87(26), 263507
[105] Du X, Zhang X, Yang Z, et al. Water oxidation catalysis beginning with $CuCo_2SO_4$: Investigation of the true electrochemically driven catalyst. Chem Asian J, 2018, 13(3), 266
[106] Peter S C. Reduction of CO_2 to chemicals and fuels: a solution to global warming and energy crisis. ACS Energy Lett, 2018, 3(7), 1557
[107] Poudyal R, Loskot P, Nepal R, et al. Mitigating the current energy crisis in Nepal with renewable energy sources. Renewable Sustainable Energy Rev, 2019, 116109388
[108] Ren Y, Sun R, Yu X, et al. A systematic study on synthesis parameters and thermoelectric properties of tellurium nanowire bundles. Mater Adv, 2023, 4(19), 4455
[109] Wu K, Ma H, Gao Y, et al. Highly-efficient heterojunction solar cells based on two-dimensional tellurene and transition metal dichalcogenides. J Mater Chem A, 2019, 7(13), 7430
[110] Lin Y, Norman C, Srivastava D, et al. Thermoelectric power generation from lanthanum strontium titanium oxide at room temperature through the addition of graphene. ACS Appl Mater Interfaces, 2015, 7(29), 15898
[111] Qin G, Yan Q B, Qin Z, et al. Hinge-like structure induced unusual properties of black phosphorus and new strategies to improve the thermoelectric performance. Sci Rep, 2014, 4(1), 6946
[112] Mettan X, Pisoni R, Matus P, et al. Tuning of the thermoelectric figure of merit of $CH_3NH_3MI_3$ (M = Pb, Sn) photovoltaic perovskites. J Phys Chem C, 2015, 119(21), 11506
[113] Meng Y, Wang W, Ho J C. One-dimensional atomic chains for ultimate-scaled electronics. ACS Nano, 2022, 16(9), 13314
[114] Meng Y, Wang W, Wang W, et al. Anti-ambipolar heterojunctions: materials, devices, and circuits. Adv Mater, 2024, 36(17), 2306290
[115] Wang W, Meng Y, Wang W, et al. Highly efficient full van der Waals 1D p-Te/2D n-Bi_2O_2Se heterodiodes with nanoscale ultraphotosensitive channels. Adv Funct Mater, 2022, 32(30), 2203003
[116] Liu Q, Wei Q, Ren H, et al. Circular polarization-resolved ultraviolet photonic artificial synapse based on chiral perovskite. Nat Commun, 2023, 14(1), 7179

Jiachi Liao got his bachelor's degree in 2023 from the Northwestern Polytechnical University and his master's degree in 2024 from the City University of Hong Kong. Currently, he is a Research Assistant at the City University of Hong Kong under the supervision of Prof. Johnny C. Ho. His research focuses on elemental tellurium nanomesh growth and characterization of related devices.

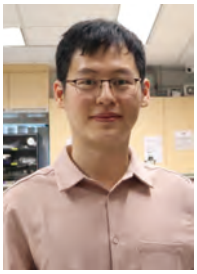

Zhengxun Lai is an Associate Professor in the College of Semiconductors at Hunan University. He received his B.S. degree in Applied Physics and M.S. degree in Materials Physics and Chemistry from Tianjin University in 2016 and 2019, respectively, and a Ph.D. degree in Materials Science and Engineering from the City University of Hong Kong in 2023. His research interests are focused on the halide perovskites electronic and photoelectric devices.

You Meng is a Postdoctoral Researcher in the Department of Materials Science and Engineering at the City University of Hong Kong. He received his B.S. degree in Applied Physics and M.S. degree in Physics from Qingdao University in 2015 and 2018, respectively, and a Ph.D. degree in Materials Science and Engineering from the City University of Hong Kong in 2021. His research interests mainly focus on nanomaterials-based electronics and optoelectronics.

Johnny C. Ho is a Professor of Materials Science and Engineering at the City University of Hong Kong. He received his B.S. degree in Chemical Engineering and his M.S. and Ph.D. degrees in Materials Science and Engineering from the University of California, Berkeley, in 2002, 2005, and 2009, respectively. From 2009-2010, he was a Postdoctoral Research Fellow in the Nanoscale Synthesis and Characterization Group at Lawrence Livermore National Laboratory. His research interests focus on the synthesis, characterization, integration, and device applications of nanoscale materials for various technological applications, including nanoelectronics, sensors, and energy harvesting.